Journal of Proteomics 205 (2019) 103417

Contents lists available at ScienceDirect

Journal of Proteomics

journal homepage: www.elsevier.com/locate/jprot

Interaction networks of Weibel-Palade body regulators syntaxin-3 and syntaxin binding protein 5 in endothelial cells

Maaike Schillemans[a,1], Ellie Karampini[a,1], Arie J. Hoogendijk[a], Maryam Wahedi[a], Floris P.J. van Alphen[b], Maartje van den Biggelaar[a], Jan Voorberg[a,c], Ruben Bierings[a,d,*]

[a] Molecular and Cellular Hemostasis, Amsterdam UMC, University of Amsterdam, The Netherlands
[b] Research Facilities, Sanquin Research and Landsteiner Laboratory, Amsterdam UMC, University of Amsterdam, The Netherlands
[c] Experimental Vascular Medicine, Amsterdam UMC, University of Amsterdam, Amsterdam, The Netherlands
[d] Hematology, Erasmus University Medical Center, Rotterdam, The Netherlands

ARTICLE INFO

Keywords:
Endothelial cells
Weibel-Palade body
SNARE protein
Syntaxin
Protein-protein interactions

ABSTRACT

The endothelium stores the hemostatic protein Von Willebrand factor (VWF) in endothelial storage organelles called Weibel-Palade bodies (WPBs). During maturation, WPBs recruit a complex of Rab GTPases and effectors that associate with components of the SNARE machinery that control WPB exocytosis. Recent genome wide association studies have found links between genetic variations in the SNAREs syntaxin-2 (*STX2*) and syntaxin binding protein 5 (*STXBP5*) and VWF plasma levels, suggesting a role for SNARE proteins in regulating VWF release. Moreover, we have previously identified the SNARE proteins syntaxin-3 and STXBP1 as regulators of WPB release. In this study we used an unbiased iterative interactomic approach to identify new components of the WPB exocytotic machinery. An interactome screen of syntaxin-3 identifies a number of SNAREs and SNARE associated proteins (STXBP2, STXBP5, SNAP23, NAPA and NSF). We show that the VAMP-like domain (VLD) of STXBP5 is indispensable for the interaction with SNARE proteins and this capacity of the VLD could be exploited to identify an extended set of novel endothelial SNARE interactors of STXBP5. In addition, an STXBP5 variant with an N436S substitution, which is linked to lower VWF plasma levels, does not show a difference in interactome when compared with WT STXBP5.

Significance: The hemostatic protein Von Willebrand factor plays a pivotal role in vascular health: quantitative or qualitative deficiencies of VWF can lead to bleeding, while elevated levels of VWF are associated with increased risk of thrombosis. Tight regulation of VWF secretion from WPBs is therefore essential to maintain vascular homeostasis. We used an unbiased proteomic screen to identify new components of the regulatory machinery that controls WPB exocytosis. Our data expand the endothelial SNARE protein network and provide a set of novel candidate WPB regulators that may contribute to regulation of VWF plasma levels and vascular health.

1. Introduction

Endothelial cells (ECs) form the inner lining of the blood vessel and actively participate hemostasis, inflammation and angiogenesis. Their characteristic secretory vesicles, called Weibel-Palade bodies (WPBs), store the hemostatic protein von Willebrand factor (VWF), along with a set of inflammatory and angiogenic proteins [1–3]. The WPB content can be released from ECs into the vascular lumen through exocytosis of these vesicles. Tight regulation of WPB exocytosis is required for vascular homeostasis and to enable a rapid response to vascular injury. Under steady state conditions, endothelial cells are involved in the maintenance of blood plasma levels of VWF through continuous, unstimulated release of WPBs via the basal secretion pathway [4,5]. Low circulating levels of VWF are associated with bleeding, such as in the inherited bleeding disorder Von Willebrand Disease (VWD), while elevated levels of VWF are linked to increased risk of thrombosis [6,7]. Upon vascular injury, however, VWF is quickly released to enable the formation of a network of VWF strings to which platelets can bind, eventually leading to platelet plug formation [8]. Along with VWF, other storage components of WPBs are released which direct leukocyte extravasation, such as P-selectin, CD63 and various chemokines, or which control angiogenesis, such as Ang-2 and IGFBP7 [1].

* Corresponding author at: Hematology, Erasmus University Medical Center, Rotterdam, The Netherlands.
E-mail address: r.bierings@erasmusmc.nl (R. Bierings).
[1] These authors contributed equally to this study.

https://doi.org/10.1016/j.jprot.2019.103417
Received 21 February 2019; Received in revised form 17 May 2019
Available online 13 June 2019

A large number of regulators of WPB trafficking and exocytosis has previously been identified. Several Rabs and Rab effectors are recruited during WPB maturation that direct trafficking and exocytosis, such as Rab27A and Rab3 isoforms and their effectors Munc13–4, MyRIP and Slp4-a [9–17]. WPB trafficking and content expulsion is further supported by actin, actin binding proteins and other regulators of the actin cytoskeleton [18–22]. Another set of regulators of WPB exocytosis are proteins of the soluble NSF attachment factor receptor (SNARE) family. SNARE proteins form a molecular complex that positions two membranes in close proximity while the mechanical force that is generated during assembly overcomes the energy barrier that prevents spontaneous membrane fusion [23]. The core of a SNARE complex is formed by the interaction of 4 alpha helices that are typically provided by 3 Q-SNARE motifs on one membrane and an R-SNARE motif on the opposing membrane. SNARE proteins contribute to the specificity of membrane fusion events and depending on the identity and the positioning of the SNAREs involved membrane fusion may occur between organelles (homotypic or heterotypic), or between (secretory) organelles and the plasma membrane, such as in exocytosis. The exocytotic SNARE complex is composed of a syntaxin (Qa) and a synaptosome associated protein 25 (SNAP25) homologue (Qbc) on the target membrane and a VAMP (R) on the secretory vesicle membrane [24]. The Q-SNAREs syntaxin-2, -3 and -4 and SNAP23 [25–29], as well as the R-SNAREs VAMP3 and VAMP8 [30,31] have all been previously implicated in WPB exocytotic processes. In addition, WPB release is regulated by STXBP1 and STXBP3 [28,32], proteins of the STXBP/SEC1/unc-18 family which in most but not all cases promote fusogenic SNARE complex formation through binding to syntaxins [33]. STXBP5 is an inhibitor of endothelial VWF release in mice and men [34] and its in vivo relevance is further underscored by human genetic polymorphisms in STXBP5 that are linked to VWF plasma levels, incidence of venous thrombosis and bleeding severity in VWD patients [25,26,35–40].

Despite the extensive (but possibly not all-encompassing) list of regulators that can be part of the WPB secretory complex, the mechanisms that control secretory processes in endothelial cells remain poorly defined. Due to our fragmented understanding of the links that are made between different components of the WPB SNARE machinery, the composition of the SNARE complex(es) that operate(s) during WPB release is currently unclear. In this study, we set out to map the SNARE interaction network involved in WPB release by performing an unbiased screen of the interactomes of two recently identified determinants of WPB exocytosis, syntaxin-3 and STXBP5. We first explored the interactome of syntaxin-3 and identified among its endothelial protein-protein interaction partners a number of SNARE proteins, including STXBP2 and STXBP5. A subsequent interactomic analysis of STXBP5 and a set of STXBP5 truncation variants identified a large number of additional Q-SNAREs, the interaction of which was dependent on the carboxyterminal VAMP-like domain (VLD) of STXBP5. Taken together, this shows that both syntaxin-3 and STXBP5 are part of a larger endothelial SNARE network, the members of which are potential novel regulators of WPB fusion events.

2. Materials and methods

2.1. Antibodies and reagents

Fetal calf serum (FCS) was from Bodinco (Alkmaar, Netherlands). Trypsin, MS grade Halt protease and phosphatase inhibitors and Alexa Fluor® 405/488/568/633/647-conjugated secondary antibodies were from Thermo Fisher Scientific (Landsmeer, Netherlands). Primary antibodies used in this study are shown in Supplementary Table 1.

2.2. DNA constructs

mEGFP-LIC, LVX-mEGFP-LIC and a lentiviral construct encoding mEGFP fused to the N-terminus of human syntaxin-3 (LVX-mEGFP-STX3) have been described previously [13,27,32]. Oligonucleotide sequences of primers used in this study are shown in Supplementary Table 2. For construction of mEGFP tagged to the N-terminus of human full length STXBP5 (residue 1–1115) the STXBP5 coding sequence was amplified with RBNL017 and RBNL018 using a human STXBP5 cDNA clone (clone ID 8322460, Thermo Scientific) as template. For construction of mEGFP-(STXBP5)VLD the VLD (1031–1115) was amplified using RBNL171 and RBNL018. For mEGFP-STXBP5ΔVLD (1 − 1030) a fragment was amplified using RBNL017 and RBNL223. The PCR products were cloned in frame behind mEGFP in the mEGFP-LIC vector by ligation independent cloning essentially as described [13]. An asparagine to serine substitution at position 436 (N436S) corresponding to the non-synonymous SNP *rs1039084* [26] was introduced in mEGFP-STXBP5 by PCR mutagenesis using RBNL138 and RBNL139. LVX-mEGFP-STXBP5, LVX-mEGFP-STXBP5-N436S, LVX-mEGFP-(STXBP5)VLD and LVX-mEGFP-STXBP5ΔVLD were constructed by insertion of *Asc*I-*Not*I fragments from mEGFP-STXBP5 (3377 bp), mEGFP-STXBP5-N436S (3377 bp), mEGFP-(STXBP5)VLD (290 bp) or mEGFP-STXBP5ΔVLD (3122 bp), respectively between the AscI and NotI site of LVX-mEGFP-LIC. All constructs were verified by sequence analysis. A schematic overview of all constructs is shown in Fig. 1.

2.3. Cell culture and lentiviral transduction

Pooled, cryo-preserved primary human umbilical vein endothelial cells (HUVECs) were obtained from Promocell (Heidelberg, Germany) and were cultured as described [32]. HUVECs were cultured in EGM-2 medium (Lonza, Basel, Switzerland) supplemented with 18% FCS (EGM-18) [32]. HEK293T cells were obtained from ATCC (Wessel, Germany) and were grown in Dulbecco's modified Eagle medium containing D-glucose, L-glutamine, and pyruvate (Life Technologies, Bleiswijk, The Netherlands) supplemented with 10% FCS, 100 U/m penicillin, and 100 mg/ml streptomycin. Lentivirus was produced in HEK293Ts using $CaCl_2$ mediated transfection of the lentiviral constructs (described above) together with 3rd generation lentiviral packaging plasmids pMD2.G, pRSV-REV and pMDLg/pRRE were purchased from (Addgene, Cambridge, USA) essentially as described [41]. After 6–8 h incubation, the medium was exchanged for EGM-18 and harvested 24–48 h later. EGM-18 with virus was filtered through 0.45 µm pore filters and virus was precipitated using polyethylene glycol 6000 and then resuspended in fresh EGM-18 at a higher concentration. Passage 6 HUVECs were transduced when at 50–80% confluency with an empirically determined amount of concentrated virus in culture medium and transduced cells were selected by 48 h incubation with 1 µg/ml

Fig. 1. Overview of the syntaxin-3 (STX3) and syntaxin-binding protein 5 (STXBP5) based constructs used in this study. All constructs were mEGFP-tagged at the N-terminus and mEGFP alone was used as a control. The constructs encode full length syntaxin-3 (mEGFP-STX3), full length wild-type STXBP5 (mEGFP-STXBP5), C-terminally truncated STXBP5 lacking its VAMP-like domain (VLD) (mEGFP-STXBP5ΔVLD), N-terminally truncated STXBP5 encoding the VLD alone (mEGFP-(STXBP5)VLD) and full length STXBP5 with an asparagine to serine substitution at position 436 (mEGFP-STXBP5-N436S).

puromycin for efficient expression of the mEGFP-tagged fusion proteins.

2.4. Immunoblotting

Proteins were separated on a Novex NuPAGE 4–12% Bis-Tris gel (ThermoFisher) and transferred onto a nitrocellulose membrane (iBlot Transfer Stack, ThermoFisher). Membranes were blocked with Odyssey blocking buffer (LI-COR Biosciences, Lincoln) and probed with primary antibodies followed by IRDye-conjugated secondary antibodies. IRDye-conjugated antibodies were visualized by LI-COR Odyssey Infrared Imaging System (LI-COR Biosciences).

2.5. Immunoprecipitation

HUVECs expressing lentivirally transduced mEGFP-fusion proteins were seeded in 3 separate wells on 6 well culture plates to enable in triplicate sample preparation for pull-downs of each condition. After 3 days of confluency, cells were rinsed 2× in PBS and subsequently lysed in mass spectrometry (MS) grade lysis buffer (10 mM Tris.HCl (pH 7.5), 150 mM NaCl, 0.5 mM EDTA, 0.5% NP40 (*v*/v)) supplemented with Halt protease and phosphatase inhibitor cocktail (Thermo Scientific). Lysates were centrifuged for 10 min at 16,000*g* and supernatants were transferred to fresh tubes. Cleared lysates were incubated with magnetic anti-GFP nanobody (nAb) beads or blocked control (CTRL) beads (Allele Biotech, San Diego, USA) by rotation for 2 h at room temperature. For interactome analysis by MS, beads were collected on a magnetic stand and were washed 3 times with wash buffer (10 mM Tris.HCl (pH 7.5), 150 mM NaCl, 0.5 mM EDTA) supplemented with Halt protease and phosphatase inhibitor cocktail (Thermo Scientific) and two times with 1 ml PBS. Further sample preparation for MS is described below. Alternatively, for analysis by immunoblotting, beads were washed four times with lysis buffer. Co-immunoprecipitates and lysates were analyzed by immunoblotting as described above.

2.6. Sample preparation for mass spectrometry analysis

Immunoprecipitated proteins were reduced on-bead in 1 M urea (Life technologies), 10 mM DTT (Thermo Scientific) in 100 mM TRIS-HCl pH 7.5 (Life technologies) for 20 min at 20 °C and alkylated with 50 mM iodoacetamide (Life technologies) for 10 min at 20 °C. Proteins were detached from the GFP-nanobody beads by incubation with 250 ng MS-grade trypsin (Promega) for 2 h at 20 °C. Beads were removed and proteins were further digested for 16 h at 20 °C with 350 ng MS-grade trypsin (Promega). Tryptic peptides were desalted and concentrated using Empore-C18 StageTips and eluted with 0.5% (*v*/v) acetic acid, 80% (v/v) acetonitrile. Sample volume was reduced by SpeedVac and supplemented with 2% acetonitrile, 0.1% TFA to a final volume of 5 µl. 3 µl of each sample was injected for MS analysis.

2.7. Mass spectrometry data acquisition

Tryptic peptides were separated by nanoscale C18 reverse phase chromatography coupled on-line to an Orbitrap Fusion Lumos Tribrid mass spectrometer (Thermo Scientific) via a nanoelectrospray ion source (Nanospray Flex Ion Source, Thermo Scientific). Peptides were loaded on a 20 cm 75–360 µm inner-outer diameter fused silica emitter (New Objective) packed in-house with ReproSil-Pur C18-AQ, 1.9 µm resin (Dr Maisch GmbH). The column was installed on a Dionex Ultimate3000 RSLC nanoSystem (Thermo Scientific) using a MicroTee union formatted for 360 µm outer diameter columns (IDEX) and a liquid junction. The spray voltage was set to 2.15 kV. Buffer A was composed of 0.5% acetic acid and buffer B of 0.5% acetic acid, 80% acetonitrile. Peptides were loaded for 17 min at 300 nl/min at 5% buffer B, equilibrated for 5 min at 5% buffer B (17–22 min) and eluted by increasing buffer B from 5 to 28% (22–80 min) and 28–40% (80–85 min), followed by a 5 min wash to 95% and a 5 min regeneration to 5%. Survey scans of peptide precursors from 375 to 1500 m/z were performed at 240 K resolution (at 200 m/z) with a 1×10^6 ion count target. Tandem MS was performed by isolation with the quadrupole with isolation window 0.7, HCD fragmentation with normalized collision energy of 30, and rapid scan MS analysis in the ion trap. The MS^2 ion count target was set to 3×10^4 and the max injection time was 20 ms. Only those precursors with charge state 2–7 were sampled for MS^2. The dynamic exclusion duration was set to 20 s with a 10 ppm tolerance around the selected precursor and its isotopes. Monoisotopic precursor selection was turned on. The instrument was run in top speed mode with 1 s cycles. All data were acquired with Xcalibur software.

2.8. Data analysis and statistics

RAW mass spectrometry files were processed with MaxQuant 1.6.0.13 using the human Uniprot database (downloaded March 2017) [42]. MaxQuant output tables were analyzed using R/Bioconductor (version 3.4.3/3.6) 'reverse', 'potential contaminants' and 'only identified by site' peptides were filtered out and label free quantification values were $\log_2$ transformed [43]. Proteins with 100% valid values in at least one experimental group were selected. Missing values were imputed by normal distribution (width = 0.3, shift = 1.8), assuming these proteins were close to the detection limit. Statistical analyses were performed using moderated *t*-tests in the LIMMA package [44]. Protein interactor significance was determined with a smooth cutoff based on the $\log_2$ fold change and *p*-value representing a 5% FDR [45]. Proteins that were statistically significant both between mEGPF-"target protein"/nAb beads versus mEGPF-"target protein"/CTRL beads and versus mEGFP/nAb beads were considered high confidence interactors. The .raw MS files and search/identification files obtained with MaxQuant have been deposited in the ProteomeXchange Consortium via the PRIDE partner repository with the dataset identifier PXD012809 [46].

Interaction networks were visualized in Cytoscape v3.6.1 and compared to previously identified interactions of human syntaxin-3 and STXBP5 imported from the BioGrid database [47].

3. Results

3.1. Syntaxin-3 interacts with several SNAREs and related proteins

The WPB regulating Qa-SNARE was initially identified together with STXBP1 in a proteomic screen for interactors of Slp4-a [32] and we have subsequently shown that syntaxin-3 forms SNARE complexes that contain the Qbc-SNARE SNAP23 together with R-SNAREs VAMP8 or (to a lesser extent) VAMP3, respectively [27]. In endothelial cells syntaxin-3 is found on WPBs and also on endosomes [27], which most probably reflects the fact that syntaxin-3, like many other SNARE proteins, continuously recycles through the endocytic pathway after having taken part in a membrane fusion event. To identify additional (regulatory) components of the WPB exocytotic machinery, we used an unbiased affinity purification-mass spectrometry (AP-MS) based approach using ectopic expression of epitope-tagged baits in endothelial cells. We anticipate that apart from SNARE proteins this unbiased approach will also identify interactors that associate with syntaxin-3 proximal or distal from the exocytotic machinery, either during re-entry from the plasma membrane after vesicle fusion or on its journey through the endocytic pathway. We cannot rule out that such interactors are indirectly relevant for secretion, for instance by correctly targeting syntaxin-3 to WPBs. mEGFP-STX3 and mEGFP (Fig. 1) were lentivirally expressed in HUVEC and immunoprecipitation (IP) of baits and interacting factors was performed using magnetic beads covalently coupled with anti-GFP nanobody (nAB) or blocked magnetic control (CTRL) beads [27]. Purified protein complexes were analyzed by MS (LC/MS-MS) after which two statistical filters were applied to exclude (1) nonspecific binders of magnetic beads (mEGFP-STX3/nAb vs

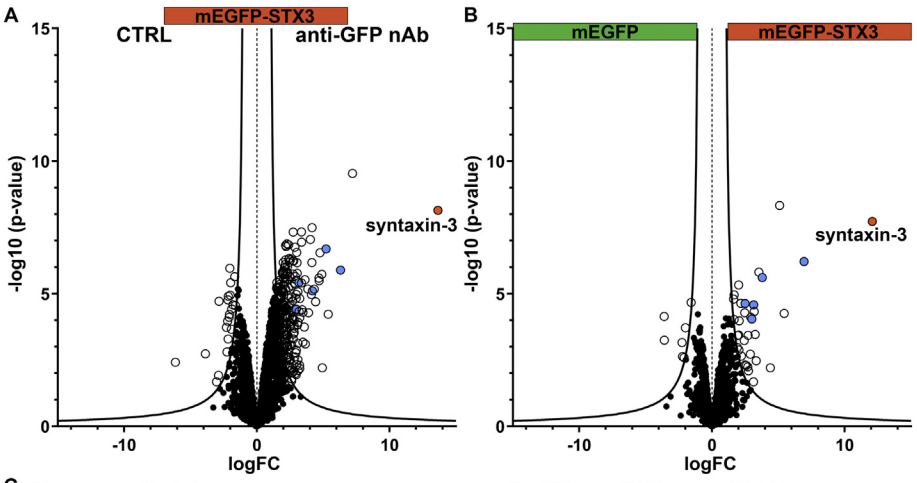

Fig. 2. Syntaxin-3 interactome is comprised of numerous SNARE related and unrelated proteins. mEGFP and mEGFP-STX3 were expressed in HUVECs and immunoprecipitated using anti-GFP nanobody (nAb) coupled beads or blocked control (CTRL) beads. A&B) Volcano plots showing differentially co-precipitated proteins when comparing mEGFP-STX3/nAb (A&B, right) vs. mEGFP-STX3/CTRL (A, left) or vs. mEGFP/nAb (B, left). The logarithmic fold-change (logFC) is shown on the x-axis and the logarithmic *p*-value (−log10 (p-value)) is shown on the y-axis. Significance cut-off line is based on an FDR of 5%. C) Table legend listing high confidence interactors of syntaxin-3 that were significantly differentiated in both control comparisons shown in A (vs. CTRL) and B (vs. mEGFP). Syntaxin-3 is depicted in orange and other SNARE complex and associated proteins are depicted in blue. (For interpretation of the references to colour in this figure legend, the reader is referred to the web version of this article.)

C

Gene	Protein	logFC: vs. CTRL	vs. mEGFP
STX3	Syntaxin-3	13.65	12.08
NSF	N-Ethylmaleimide Sensitive Factor	6.30	6.94
EML3	Echinoderm Microtubule Associated Protein Like 3	5.38	5.44
GLG1	Golgi Glycoprotein 1	7.21	5.09
STXBP2	Syntaxin Binding Protein 2	5.22	3.79
SCO1	Cytochrome C Oxidase Assembly Protein	3.58	3.26
TBK1	TANK Binding Kinase 1	3.19	3.18
NAPA	NSF Attachment Protein Alpha	2.98	3.14
SNAP23	Synaptosome Associated Protein 23	4.18	3.00
CSNK1G1	Casein Kinase 1 Gamma 1	2.84	2.93
EIF4A2	Eukaryotic Translation Initiation Factor 4A2	2.94	2.89
STXBP5	Syntaxin Binding Protein 5	3.17	2.49
FRMD5	FERM Domain Containing 5	3.62	2.47
ATP5SL	Distal Membrane Arm Assembly Complex 2	1.95	2.04
AUP1	Lipid Droplet Regulating VLDL Assembly Factor	1.90	1.91
ABCF3	ATP Binding Cassette Subfamily F Member 3	1.85	1.68
CD93	CD93 Molecule	2.86	1.67
PKN3	Protein Kinase N3	4.76	-1.99
MP68	ATP Synthase Membrane Subunit 6.8PL	-2.26	-3.60

mEGFP-STX3/CTRL) and (2) interactors of the mEGFP tag (mEGFP-STX3/nAb vs. mEGFP/nAb) (Fig. 2A–B). We confirmed the presence of our bait syntaxin-3 itself to be significantly more abundant in the mEGFP-STX3/nAb samples compared to both controls (Fig. 2). A set of high confidence interactors of syntaxin-3 was identified, including the SNARE(−associated) proteins SNAP23, N-ethylmaleimide-sensitive factor (NSF), NSF Attachment Protein Alpha (SNAP-α or NAPA), STXBP2 and STXBP5 (Fig. 2C). Syntaxin-3 interactions with SNAP23, STXBP2 and STXBP5 have previously been observed in human cells, as reported in the BioGrid database [47]. STXBP2, which has not previously been implicated in endothelial secretory processes, is a regulator of platelet alpha- and dense granule secretion [48]. Interestingly, mutations in *STXBP2* cause familial hemophagocytic lymphohistiocytosis type 5 (FHL5) and microvillous inclusion disease (MVID), the latter of which is also associated with loss of function mutations in *STX3* [49]. Additional high confidence interactors included two cytoskeleton related proteins, FERM Domain Containing 5 (FRMD5) and Echinoderm Microtubule Associated Protein Like 3 (EML3), which have not been previously associated with syntaxin-3. Interestingly, golgi glycoprotein 1 (GLG1) and CD93, two transmembrane proteins that are involved in leukocyte-endothelial adhesion, were also identified as syntaxin-3 partners. GLG1, one of the most prominent endothelial interactors of syntaxin-3 from this screen (also Supplementary Fig. 1), is a ligand of the endothelial adhesion molecule *E*-selectin and is primarily found on leukocyte microvilli [50]. Both CD93 and GLG1 are cell surface molecules that are recycled after endocytosis, which could mean these interactions take place when syntaxin-3 arrives on the plasma membrane after exocytosis, or after internalization when they coexist with syntaxin-3 in endosomes. Altogether, we identified a large set high confidence syntaxin-3 interactors, including several SNARE proteins, which could be novel regulators of WPB trafficking and exocytosis.

3.2. The carboxyterminal VAMP-like domain of STXBP5 is sufficient and indispensable for SNARE protein interaction

One SNARE associated hit from our syntaxin-3 interaction screen was the syntaxin binding protein STXBP5. STXBP5 has been classified as an R-SNARE protein because of its C-terminal VLD which contains an R-SNARE motif that enables its binding to syntaxin-1 [51–53]. Two recent reports have shown that STXBP5 regulates VWF release from platelets and endothelial cells through interaction with, respectively, syntaxin-11/SNAP23 and syntaxin-4/SNAP23 complexes [34,54], which highlights STXBP5's promiscuity in Q-SNARE interactions. To further focus on how STXBP5 partakes in endothelial SNARE-mediated VWF secretion a number of STXBP5 variants were designed with which we addressed the role of the VLD in endothelial STXBP5-SNARE interactions (Fig. 1). mEGFP-tagged full length STXBP5 (mEGFP-STXBP5), an N-terminal variant lacking the carboxyterminal VLD (mEGFP-STXBP5ΔVLD) and a variant comprised of the VLD alone (mEGFP-(STXBP5)VLD) were expressed in HUVECs (Supplementary Fig. 2) and we used a similar AP-MS based approach as described above to perform an unbiased screen for high confidence interactors of these three STXBP5 variants. A limited set of high confidence interactors was identified for mEGFP-STXBP5 full length when compared to mEGFP, which included the SNARE proteins, NSF, syntaxin-12 and NAPA (Fig. 3A&E, Supplementary Fig. 3A). Notably, the truncated mEGFP-

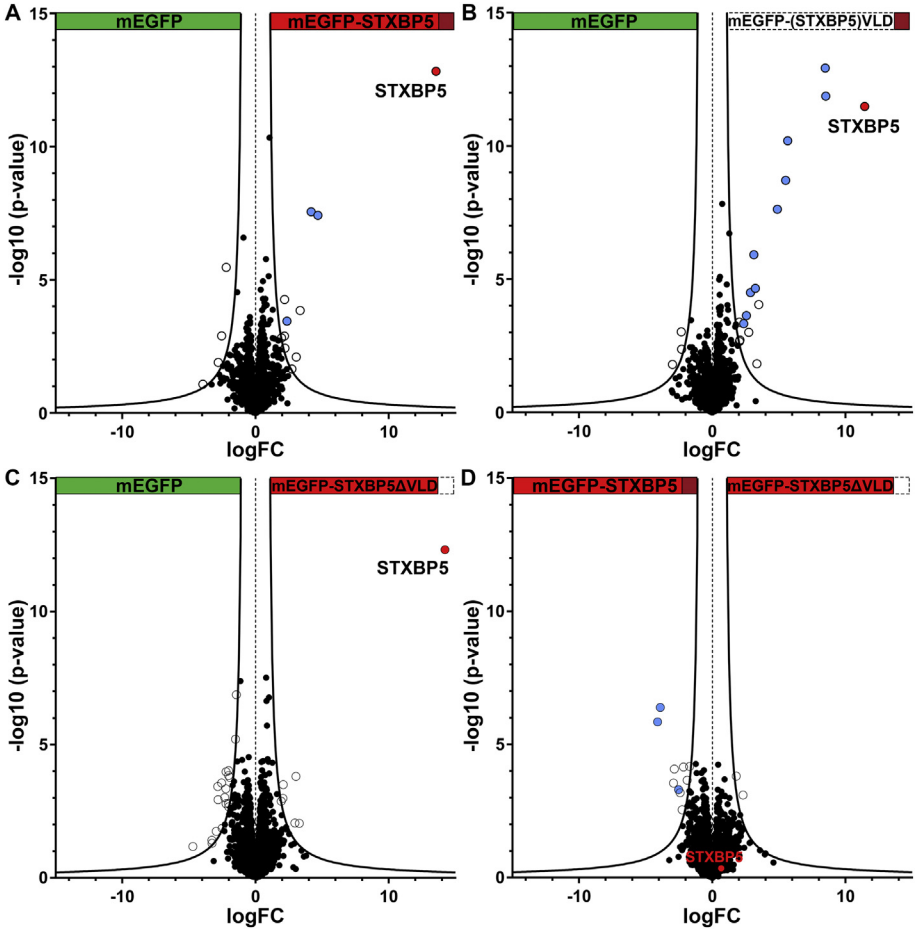

Fig. 3. Syntaxin-binding protein 5 (STXBP5) interacts with a number of SNAREs through its VAMP-like domain (VLD). mEGFP-tagged STXBP5 variants and mEGFP (see schematic overview in Fig. 1) were expressed in HUVECs and immunoprecipitated using anti-GFP nanobody coupled beads. A-D) Volcano plots showing differentially co-precipitated proteins when comparing mEGFP-STXBP5 (A), mEGFP-(STXBP5)VLD (B) or mEGFP-STXBP5ΔVLD (C) vs. mEGFP and mEGFP-STXBP5ΔVLD vs. mEGFP-STXBP5 (D). The logarithmic fold-change (logFC) is shown on the x-axis and the logarithmic p-value (−log10 (p-value)) is shown on the y-axis. Significance cut-off line is based on an FDR of 5%. *E*-G) Table legends listing high confidence interactors of the STXBP5 variants that were significantly differentiated in both control comparisons shown respectively in panels A-C of this figure (vs. mEGFP) and of Supplementary Fig. 3 (vs. CTRL). H) Table legend listing significantly differentiated interactors when comparing mEGFP-STXBP5ΔVLD vs. mEGFP-STXBP5 (panel B) after filtering for significant(*) co-precipitators of either mEGFP-STXBP5 (Supplementary Fig. 3) or mEGFP-STXBP5ΔVLD (Supplementary Fig. 3) vs. their corresponding blocked control beads (vs. CTRL). STXBP5 is depicted in red and other SNARE complex and associated proteins are depicted in blue. (For interpretation of the references to colour in this figure legend, the reader is referred to the web version of this article.)

STXBP5ΔVLD showed a complete loss of high confidence interactors, including all SNAREs (Fig. 3C&G and Fig. 5B, Supplementary Fig. 3C). Since the level of expression of the smaller mEGFP construct differs from the larger mEGFP-STXBP5 and mEGFP-STXBP5ΔVLD constructs (Fig. 4) this may have resulted in substantial differences between the amount of bait present in our samples, which could have skewed the outcome of our analysis. For this reason we also carried out a direct comparison between the full length and ΔVLD constructs which were expressed at similar levels. High confidence interactors were identified by selecting co-precipitators that were (1) significantly more abundant in co-precipitations of either of these constructs, and (2) also significantly more abundant compared to their respective CTRL bead condition (Fig. 3D&H and Supplementary Fig. 3A&C). In agreement with the results from their separate analyses, the SNARE proteins NSF, NAPA and syntaxin-12 were also identified as high confidence interactors of mEGFP-STXBP5 full length, while no specific interactors were found for the N-terminal variant mEGFP-STXBP5ΔVLD. This implies that the SNARE interactors of STXBP5 were exclusively supported by the VLD domain. To further characterize the syntaxin binding capacity of the VLD and possibly identify additional STXBP5 interactors, we also mapped the interactors of the isolated VLD moiety (mEGFP-(STXBP5) VLD; Fig. 3B&F, Supplementary Fig. 3B). This led to an extended list of SNAREs(−related) interactors, including several syntaxins (syntaxin-4, −7, −8 and −12), and other SNARE complex proteins (SNAP23, SNAP29, NAPA and NSF). Furthermore we also identified the ER-Golgi Sec1/unc18 protein SCFD1 (also Sly1 or STXBP1L2) [55] and a member of the ER-associated NRZ tethering complex, NBAS/NAG, which regulates assembly of ER Q-SNAREs [56].

In contrast to most R-SNAREs and syntaxin-binding proteins, which promote membrane fusion, STXBP5 has been shown to inhibit exocytosis [57–64]. Cumulative evidence suggests that this inhibitory role for STXBP5 is mediated by its capacity to bind to syntaxins through its VLD, which competes with VAMPs during the formation of SNARE complexes [61,65]. This raises the possibility that STXBP5 controls VWF plasma levels through inhibition of SNARE-mediated WPB fusion by displacing VAMPs and sequestering syntaxins into non-fusogenic dead ends. To test this we studied the interaction of STXBP5 variants with syntaxin-2, -3, -4, and SNAP23, Q-SNARE proteins that are expressed in endothelial cells and which all have been previously related to plasma VWF levels or regulation of WPB release [27–29,36]. In agreement with the SNARE interaction data from our unbiased screens, we found that full length STXBP5 interacts with all of these specific

E

Gene	Protein	mEGFP-STXBP5 logFC: vs. CTRL	vs. mEGFP
STXBP5	Syntaxin binding protein 5	13.46	13.55
NSF	N-Ethylmaleimide Sensitive Factor, Vesicle Fusing	4.65	4.68
STX12	Syntaxin 12	4.45	4.17
MSH3	DNA mismatch repair protein Msh3	3.04	3.05
NAPA	NSF Attachment Protein Alpha	3.00	2.35
HEATR1	HEAT repeat-containing protein 1	-2.31	-2.21

F

Gene	Protein	logFC:	mEGFP-(STXBP5)VLD vs. CTRL	vs. mEGFP
STXBP5	Syntaxin binding protein 5		12.94	11.44
NSF	N-Ethylmaleimide Sensitive Factor		8.52	8.51
STX12	Syntaxin 12		8.88	8.47
SNAP23	Synaptosome Associated Protein 23		5.27	5.65
STX7	Syntaxin 7		4.69	5.51
NAPA	NSF Attachment Protein Alpha		5.85	4.88
STX4	Syntaxin-4		3.14	3.24
SNAP29	Synaptosome Associated Protein 29		3.03	3.12
NBAS	Neuroblastoma Amplified Sequence		3.14	2.87
SCFD1	Sec1 Family Domain Containing 1 (STXBP1L2)		2.49	2.56
STX8	Syntaxin-8		2.00	2.36
POLR2E	RNA Polymerase II Subunit E		-2.51	-2.31
KIF3C	Kinesin Family Member 3C		-4.11	-3.00

G

Gene	Protein	mEGFP-STXBP5ΔVLD logFC: vs. CTRL	vs. mEGFP
STXBP5	Syntaxin binding protein 5	17.14	14.21
SYT11	Synaptotagmin 11	-2.04	-2.32
ATP5J	ATP synthase-coupling factor 6	-2.22	-2.55
RPL37	Ribosomal Protein L37	-3.37	-3.27

H

Gene	Protein	logFC:	mEGFP-STXBP5ΔVLD vs. mEGFP-STXBP5 WT vs. CTRL	ΔVLD vs. CTRL	ΔVLD vs WT
PPFIBP2	PPFIA Binding Protein 2		3.14	0.11	-2.26
NAPA	NSF Attachment Protein Alpha		3.00	0.65	-2.54
EWSR1	EWS RNA Binding Protein 1		2.70	-1.16	-2.92
STX12	Syntaxin 12		4.45	-0.15	-3.91
NSF	N-Ethylmaleimide Sensitive Factor		4.65	0.62	-4.11

Fig. 3. (*continued*)

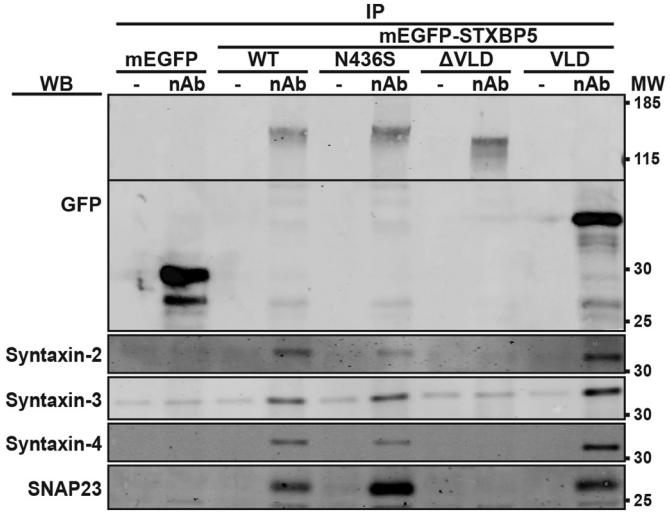

Fig. 4. Syntaxin-binding protein 5 (STXBP5) interacts with syntaxin-2, −3 and − 4 and SNAP23 through its VAMP-like domain (VLD). mEGFP-tagged STXBP5 variants and mEGFP (see schematic overview in Fig. 1) were lentivirally expressed in HUVEC and immunoprecipitated using anti-GFP nanobody coupled beads (+) or blocked control beads (−). Immunoblots of lysates (input) and co-immunoprecipitates (IP) were probed with anti-GFP, anti-SNAP23, anti-syntaxin-2, anti-syntaxin-3, or anti-syntaxin-4. Molecular weight (MW) marker bands are shown on the right.

SNARE targets, but the interaction is lost upon deletion of the VLD (Fig. 4). In contrast, the VLD alone appeared to be sufficient for their binding. Altogether this has added several novel endothelial partners to the previously reported interactors of STXBP5 (Fig. 5A), which are potential downstream targets in STXBP5-mediated VWF secretion.

3.3. The N436S point mutation does not lead to a change in interactome

Our finding that the VLD moiety enables STXBP5 to engage in SNARE complex formation with all exocytotic Q-SNAREs that are relevant in WPB release, suggests that interactions with these SNAREs are at the basis of the inhibitory function of STXBP5 in VWF secretion from endothelial cells [34]. The minor allele of the common STXBP5 polymorphism *rs1039084* encodes for the non-synonymous point mutation Asp436Ser (N436S), which is located in the N-terminal domain of STXBP5, i.e. outside of the VLD. The N436S substitution has been linked to lower plasma VWF levels, decreased incidence of venous thrombosis and increased bleeding in female VWD patients [26,36,40], a phenotype that was recapitulated in CRISPR/Cas9-engineered mice carrying the orthologous human mutation (N437S) [66]. This means the N436S substitution potentiates the inhibitory action of STXBP5, as was also observed in vitro [34], however, little is known about the underpinning molecular mechanism. A possible scenario would involve gain or loss of specific interactors that determine the efficacy of STXBP5-mediated inhibition of SNARE complex formation. To investigate whether the substitution alters binding of STXBP5 with its interaction partners, we used an mEGFP-tagged STXBP5 variant

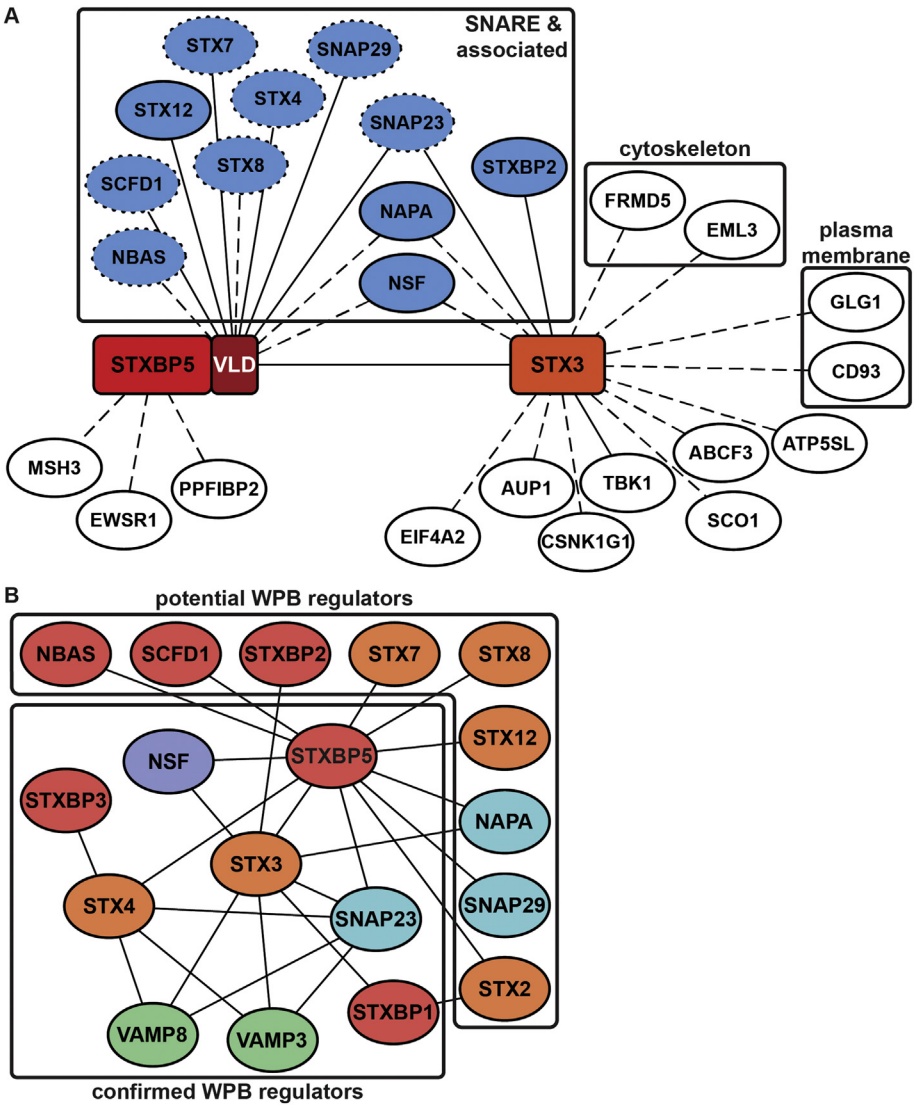

Fig. 5. Interaction networks of syntaxin binding protein 5 and syntaxin-3 in endothelial cells. A) Interaction network showing individual and shared interactors of syntaxin binding protein 5 (STXBP5) and syntaxin-3 (STX3). Dashed lines show newly found interactions and solid lines show interactions that have previously been identified in human cells and were reported in the BioGRID database. For STXBP5, SNAREs and associated proteins (blue) all interacted through the VAMP-like domain (VLD): nodes with a solid edge represent interactors that coprecipitated with mEGPF-STXBP5 and nodes with a dotted edge represent interactors that coprecipicated with mEGFP-VLD only. B) Overview of previously and newly identified SNARE protein interactions in endothelial cells. Proteins are classified as confirmed or as potential regulators of WPB trafficking and release. Colors indicate syntaxins (orange), SNARE accessory proteins (red), VAMPs (green), SNAPs (blue) and NSF (purple). (For interpretation of the references to colour in this figure legend, the reader is referred to the web version of this article.)

carrying the N436S substitution (mEGFP-STXBP5-N436S). We identified high confidence interactors using a similar AP-MS based approach as described above. We observed a similar SNARE interaction pattern as for wild-type STXBP5, with the addition of syntaxin-8, however it must be noted that this interaction was just above the significance cut-off line (Fig. 6A&C, Supplementary Fig. 3D). When directly comparing interactors of mEGFP-STXBP5-N436S with mEGFP-STXBP5, no significantly different SNARE proteins were identified (Fig. 6B&D, Supplementary Fig. 3A&D). Targeted testing of the interaction of STXBP5-N436S with WPB exocytotic SNAREs also did not show changes in WPB SNARE interaction partners of this variant (Fig. 3). In conclusion, our findings do not lend support to a model where the N436S substitution affects the (SNARE) interaction capacity of STXBP5.

4. Discussion and conclusions

We used an unbiased interactomics approach to identify SNARE protein regulatory interactions that are potentially involved in WPB exocytosis. We identified a set of high confidence interactors of syntaxin-3 and STXBP5 (Fig. 5A) that, together with previously established links, provides the outline of a network of SNAREs and regulators that control VWF secretion (Fig. 5B).

We previously identified syntaxin-3 as a positive regulator of VWF release from endothelial cells that is localized on WPBs [27]. A prominent hit from our interactomic screen of syntaxin-3 was STXBP5. STXBP5, which is a central node in the WPB SNARE network, is generally an inhibitor of SNARE complex formation and exocytosis, in a variety of neuroendocrine cells [57,65,67], and this also applies for VWF secretion from endothelial cells [34]. However, STXBP5 was also reported to promote exocytosis of granules from platelets [34,54] suggesting that STXBP5 may exert pleiotropic effects in different cells. The interaction between syntaxin-3 and STXBP5 in human cells has previously been reported both in a large interaction screen of HA-FLAG tagged proteins in HEK293 cells, as well as in a mechanistic study of the function of endogenous STXBP5 in mast cells [68,69]. In the latter study, an explanation is provided for the apparently contradictory functions of STXBP5 in granule exocytosis. Madera-Salcedo and coworkers show that in resting mast cells non-phosphorylated STXBP5 preferably binds syntaxin-4, which we also identified as endothelial STXBP5 interactor, and prevents it from binding its cognate SNARE partner. Upon stimulation of the mast cells STXBP5 becomes phosphorylated which promotes its binding to syntaxin-3, enabling syntaxin-4 to form a SNARE complex and facilitate exocytosis [69]. The authors suggest that syntaxin-3 is not a direct facilitator of exocytosis, but rather acts through sequestering of STXBP5. As STXBP5 has been shown to have a preference for syntaxin-SNAP23 binding compared to syntaxin alone, they also suggest that a relocation of SNAP23 from syntaxin-4 to syntaxin-3 may occur simultaneously, such as previously

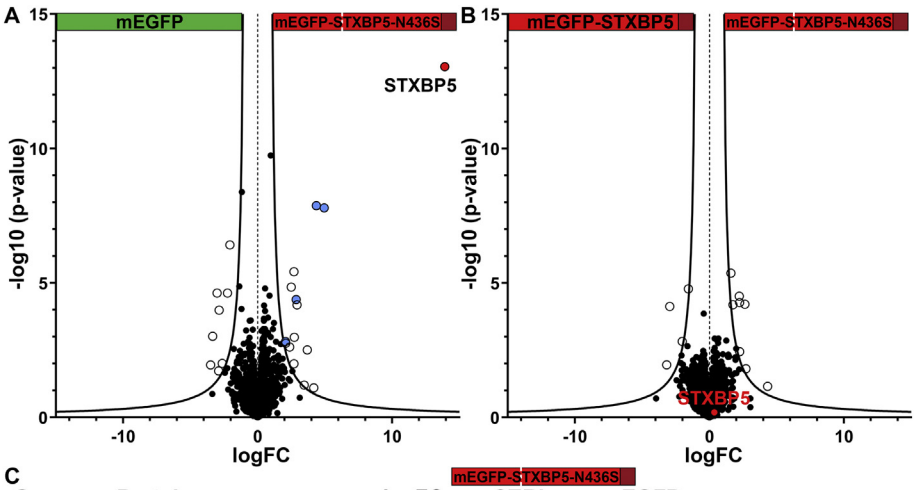

C

Gene	Protein	mEGFP-STXBP5-N436S logFC: vs. CTRL	vs. mEGFP
STXBP5	Syntaxin binding protein 5	14.02	13.91
NSF	N-Ethylmaleimide Sensitive Factor	4.47	4.94
STX12	Syntaxin 12	4.10	4.37
KIF5A	Kinesin Family Member 5A	3.82	3.45
NAPA	NSF Attachment Protein Alpha	3.82	2.87
STX8	Syntaxin-8	2.07	2.07
KRAS	KRAS Proto-Oncogene, GTPase	-1.73	-2.07
CDKL5	Cyclin Dependent Kinase Like 5	-2.80	-2.90
DPYSL2	Dihydropyrimidinase Like 2	-2.27	-3.02
NUP107	Nucleoporin 107	-3.49	-3.35

D

Gene	Protein	mEGFP-STXBP5-N436S vs. mEGFP-STXBP5 logFC: WT vs. CTRL	N436S vs. CTRL	N436S vs. WT
SMTN	Smoothelin	1.67	3.95	2.71
EWSR1	RNA-binding protein EWS	2.69	-0.22	-2.95

Fig. 6. Syntaxin binding protein 5 (STXBP5) with point mutation N436S has a similar interactome as wild-type STXBP5. mEGFP-STXBP5 and mEGFP-STXBP5-N436S (see schematic overview in Fig. 1) were expressed in HUVECs and immunoprecipitated using anti-GFP nanobody coupled beads. A-B) Volcano plots showing differentially co-precipitated proteins with mEGFP-STXBP5-N436S vs. mEGFP (A) and mEGFP-STXBP5-N436S vs. mEGFP-STXBP5 (B). The logarithmic fold-change (logFC) is shown on the x-axis and the logarithmic p-value (−log10 (p-value)) is shown on the y-axis. Significance cut-off line is based on an FDR of 5%. C) Table legend listing high confidence interactors of STXBP5-N436S that were significantly differentiated in both control comparisons shown in panel A of this figure (vs. mEGFP) and of Supplementary Fig. 3 (vs. CTRL). D) Table legend listing significantly differentiated interactors when comparing mEGFP-STXBP5-N436S vs. mEGFP-STXBP5 (panel B) after filtering for significant(*) co-precipitators of either mEGFP-STXBP5 (Supplementary Fig. 3A) or mEGFP-STXBP5-N436S (Supplementary Fig. 3D) vs. their corresponding blocked control beads (vs. CTRL). STXBP5 is depicted in red and other SNARE complex and associated proteins are depicted in blue. (For interpretation of the references to colour in this figure legend, the reader is referred to the web version of this article.)

observed in adipocytes [70]. This would be in line with our observation that STXBP5 interacts with SNAP23, however, in unstimulated endothelial cells we already observe that syntaxin-3 can interact with both STXBP5 and SNAP23. In agreement with this observation we previously identified syntaxin-3 as a WPB-localized, positive regulator of VWF release that forms SNARE complexes with VAMP8 and SNAP23 [27]. This suggests that syntaxin-3 directly promotes exocytosis of WPBs and that its role in endothelial cells is not linked to sequestering of STXBP5 to allow for syntaxin-4 mediated WPB release. However, we cannot rule out that a gradual redistribution of STXBP5 from syntaxin-4 to syntaxin-3 (or between any of the other SNAREs that were identified in this study) can fine tune the exocytotic response by giving more prominence to specific SNARE assemblies. Future studies should reveal whether a SNARE-switch controlled by the phosphorylation of STXBP5 is involved in stimulus-induced WPB release.

Our data show that the VLD or STXBP5 is required and sufficient for interaction with multiple SNAREs. The VLD has initially been identified as the minimal SNARE binding domain and was implicated in the inhibition of SNARE complex formation and exocytosis in cell free assays [52,57,60,65,70]. Other studies, on the other hand, have suggested that the N-terminal domain is also required for and capable of SNARE binding, and it has been implicated in the oligomerization of SNARE complexes. The N-terminal domain includes structural motifs called WD40 repeats, which are generally known to function as binding scaffolds that coordinate multi-protein complex assemblies [60,71]. In neurons and neuroendocrine cells, for example, the N-terminus of STXBP5 alone has been shown to be able to inhibit neurotransmitter release [60,63,72]. Our data do not support a similar mechanism in endothelial cells, as with the VLD alone we were able to pull down a large set of SNARE interactors, whereas we did not identify any SNARE interactors when a truncated N-terminal STXBP5 variant lacking the VLD was used (Fig. 3&Fig. 4). It must be noted that most of the above mentioned studies did not show direct binding of SNAREs to the STXPB5 N-terminal domains, raising the possibility that these domains may act as a regulator of SNARE binding to the VLD. The increased number of SNAREs and SNARE regulators that were identified when we used the VLD alone suggests that this moiety binds SNAREs more efficiently on its own than when it's part of the full-length STXBP5. Although we cannot rule out that difference in expression levels of our bait proteins may have contributed to this, it could also have been caused by an auto-inhibitory confirmation in which the N-terminal part of STXBP5 prevents efficient SNARE binding to the VLD. It would be interesting to investigate the potential regulatory role of these domains in WPB exocytosis.

Several studies have shown a relation between SNP *rs1039084*, which leads to a N436S substitution in the N-terminal domain of STXBP5, and lower VWF levels in plasma [26,40]. The functional data presented so far are consistent with a model in which this substitution potentiates the inhibitory function of STXBP5 [34,66]. Hence, we hypothesized that the N436S mutation may have an increased SNARE inhibitory capacity through altered protein interaction properties, especially since this mutation is located in one of the WD40 repeats. We did not see any notable differences between the interactomes of STXBP5 and STXBP5-N436S. One explanation for this could be that our interactomic studies were performed in resting cells and not under stimulated conditions. Potentially, we could have missed activation dependent differences between the interactomes of STXBP5 and STXBP5-N436S. Data from a study in chromaffin cells suggested that the N-terminal domain of STXBP5 can bind the Ca^{2+} sensor synaptotagmin 1, while at the same time the VLD can bind the neuroendocrine SNAP23 homologue SNAP25 and syntaxin-1 in a Ca^{2+}-dependent manner [63]. In contrast, another study identified syntaxin-1, SNAP25 and

synaptotagmin 1 as steady state interactors of STXBP5 in mouse synaptosomes [73]. Synaptotagmin 1 is also expressed in endothelial cells and binds STXBP5 in an activation-dependent manner [34], but the functional importance of this interaction is still unclear. A recent study has now shown that not synaptotagmin 1, but rather the WPB-localized synaptotagmin 5 is the Ca^{2+} sensor that drives WPB exocytosis [74]. Whether a physical or functional link between synaptotagmin 5 and STXBP5 is involved in WPB release remains to be determined.

In conclusion, our study provides a rough map of SNARE interactions that can contribute to regulation of WPB exocytosis (Fig. 5B). While some SNAREs may (also) be involved in other endothelial membrane fusion events, we speculate that among the extended list of SNARE and associated proteins a number of new regulators of WPB release and/or genetic loci that determine VWF levels can be found. The broad range of SNAREs that bind STXBP5 by virtue of its VLD suggests that this protein represents a main switch that can regulate numerous SNARE complex assemblies at the same time. Although additional studies would be required, we speculate that STXBP5 acts as a brake on membrane fusion events in resting endothelial cells, and that this brake is relieved upon cellular activation.

Author contributions

MS, EK, MW, FvA, AH, MvdB and RB performed research and analyzed data; MvdB, JV and RB designed the research; MS, JV and RB wrote the paper.

Funding

This study was supported by grants from the Landsteiner Stichting voor Bloedtransfusie Research (LSBR-1244, LSBR-1517 and LSBR-1707), the Netherlands Ministry of Health (PPOC-2015-24P and PPOC-2018-21) and a Research Fellowship from the European Hematology Association (EHA).

Declaration of Competing Interests

The authors report no disclosures.

Appendix A. Supplementary data

Supplementary data to this article can be found online at https://doi.org/10.1016/j.jprot.2019.103417.

References

[1] M. Schillemans, E. Karampini, M. Kat, R. Bierings, Exocytosis of Weibel-Palade bodies: how to unpack a vascular emergency kit, J. Thromb. Haemost. 17 (2019) 6–18, https://doi.org/10.1111/jth.14322.
[2] P.J. Lenting, O.D. Christophe, C.V. Denis, von Willebrand factor biosynthesis, secretion, and clearance: connecting the far ends, Blood 125 (2015) 2019–2028, https://doi.org/10.1182/blood-2014-06-528406.
[3] D.J. Metcalf, T.D. Nightingale, H.L. Zenner, W.W. Lui-Roberts, D.F. Cutler, Formation and function of Weibel-Palade bodies, J. Cell Sci. 121 (2008) 19–27, https://doi.org/10.1242/jcs.03494.
[4] J.P. Giblin, L.J. Hewlett, M.J. Hannah, Basal secretion of von Willebrand factor from human endothelial cells, Blood 112 (2008) 957–964, https://doi.org/10.1182/blood-2007-12-130740.
[5] M. Lopes da Silva, D.F. Cutler, von Willebrand factor multimerization and the polarity of secretory pathways in endothelial cells, Blood 128 (2016) 277–285, https://doi.org/10.1182/blood-2015-10-677054.
[6] F.W.G. Leebeek, J.C.J. Eikenboom, Von Willebrand's disease, N. Engl. J. Med. 375 (2016) 2067–2080, https://doi.org/10.1056/NEJMra1601561.
[7] J.E. Sadler, von Willebrand factor: two sides of a coin, J. Thromb. Haemost. 3 (2005) 1702–1709, https://doi.org/10.1111/j.1538-7836.2005.01369.x.
[8] K. De Ceunynck, S.F. De Meyer, K. Vanhoorelbeke, Unwinding the von Willebrand factor strings puzzle, Blood 121 (2013) 270–277, https://doi.org/10.1182/blood-2012-07-442285.
[9] M.J. Hannah, A.N. Hume, M. Arribas, R. Williams, L.J. Hewlett, M.C. Seabra, D.F. Cutler, Weibel-Palade bodies recruit Rab27 by a content-driven, maturation-dependent mechanism that is independent of cell type, J. Cell Sci. 116 (2003) 3939–3948, https://doi.org/10.1242/jcs.00711jcs.00711 (pii).
[10] M. Knop, E. Aareskjold, G. Bode, V. Gerke, Rab3D and annexin A2 play a role in regulated secretion of vWF, but not tPA, from endothelial cells, EMBO J. 23 (2004) 2982–2992, https://doi.org/10.1038/sj.emboj.7600319.
[11] T.D. Nightingale, K. Pattni, A.N. Hume, M.C. Seabra, D.F. Cutler, Rab27a and MyRIP regulate the amount and multimeric state of VWF released from endothelial cells, Blood 113 (2009) 5010–5018 (doi:blood-2008-09-181206 [pii] 10.1182/blood-2008-09-181206).
[12] I. Rojo Pulido, T.D. Nightingale, F. Darchen, M.C. Seabra, D.F. Cutler, V. Gerke, Myosin Va acts in concert with Rab27a and MyRIP to regulate acute von-Willebrand factor release from endothelial cells, Traffic 12 (2011) 1371–1382, https://doi.org/10.1111/j.1600-0854.2011.01248.x.
[13] R. Bierings, N. Hellen, N. Kiskin, L. Knipe, A.-V. Fonseca, B. Patel, A. Meli, M. Rose, M.J. Hannah, T. Carter, The interplay between the Rab27A effectors Slp4-a and MyRIP controls hormone-evoked Weibel-Palade body exocytosis, Blood 120 (2012) 2757–2767, https://doi.org/10.1182/blood-2012-05-429936.
[14] S. Zografou, D. Basagiannis, A. Papafotika, R. Shirakawa, H. Horiuchi, D. Auerbach, M. Fukuda, S. Christoforidis, A complete Rab screening reveals novel insights in Weibel-Palade body exocytosis, J. Cell Sci. 125 (2012) 4780–4790, https://doi.org/10.1242/jcs.104174.
[15] D. van Breevoort, E.L. van Agtmaal, B.S. Dragt, J.K. Gebbinck, I. Dienava-Verdoold, A. Kragt, R. Bierings, A.J.G. Horrevoets, K.M. Valentijn, J.C. Eikenboom, M. Fernandez-Borja, A.B. Meijer, J. Voorberg, Proteomic screen identifies IGFBP7 as a novel component of endothelial cell-specific Weibel-Palade bodies, J. Proteome Res. 11 (2012) 2925–2936, https://doi.org/10.1021/pr300010r.
[16] I.L. Conte, N. Hellen, R. Bierings, G.I. Mashanov, J.-B. Manneville, N.I. Kiskin, M.J. Hannah, J.E. Molloy, T. Carter, Interaction between MyRIP and the actin cytoskeleton regulates Weibel-Palade body trafficking and exocytosis, J. Cell Sci. 129 (2016) 592–603, https://doi.org/10.1242/jcs.178285.
[17] T. Chehab, N.C. Santos, A. Holthenrich, S.N. Koerdt, J. Disse, C. Schuberth, A.R. Nazmi, M. Neeft, H. Koch, K.N.M. Man, S.M. Wojcik, T.F.J. Martin, P. van der Sluijs, N. Brose, V. Gerke, A novel Munc13-4/S100A10/annexin A2 complex promotes Weibel-Palade body exocytosis in endothelial cells, Mol. Biol. Cell 28 (2017) 1688–1700, https://doi.org/10.1091/mbc.E17-02-0128.
[18] T.D. Nightingale, I.J. White, E.L. Doyle, M. Turmaine, K.J. Harrison-Lavoie, K.F. Webb, L.P. Cramer, D.F. Cutler, Actomyosin II contractility expels von Willebrand factor from Weibel-Palade bodies during exocytosis, J. Cell Biol. 194 (2011) 613–629, https://doi.org/10.1083/jcb.201011119.
[19] K.W.E.M. van Hooren, D. van Breevoort, M. Fernandez-Borja, A.B. Meijer, J. Eikenboom, R. Bierings, J. Voorberg, Phosphatidylinositol-3,4,5-triphosphate-dependent Rac exchange factor 1 regulates epinephrine-induced exocytosis of Weibel-Palade bodies, J. Thromb. Haemost. 12 (2014) 273–281, https://doi.org/10.1111/jth.12460.
[20] X. Han, P. Li, Z. Yang, X. Huang, G. Wei, Y. Sun, X. Kang, X. Hu, Q. Deng, L. Chen, A. He, Y. Huo, D. Li, E. Betzig, J. Luo, Zyxin regulates endothelial von Willebrand factor secretion by reorganizing actin filaments around exocytic granules, Nat. Commun. 8 (2017) 14639, , https://doi.org/10.1038/ncomms14639.
[21] P. Li, G. Wei, Y. Cao, Q. Deng, X. Han, X. Huang, Y. Huo, Y. He, L. Chen, J. Luo, Myosin IIa is critical for cAMP-mediated endothelial secretion of von Willebrand factor, Blood. 131 (2018) 686–698, https://doi.org/10.1182/blood-2017-08-802140.
[22] M. Mietkowska, C. Schuberth, R. Wedlich-Söldner, V. Gerke, Actin dynamics during Ca2+ −dependent exocytosis of endothelial Weibel-Palade bodies, Biochim. Biophys. Acta, Mol. Cell Res. (2018) 0–1, https://doi.org/10.1016/j.bbamcr.2018.11.010.
[23] R. Jahn, R.H. Scheller, SNAREs–engines for membrane fusion, Nat. Rev. Mol. Cell Biol. 7 (2006) 631–643, https://doi.org/10.1038/nrm2002.
[24] T.C. Südhof, J. Rizo, Synaptic vesicle exocytosis, Cold Spring Harb. Perspect. Biol. 3 (2011) a005637, https://doi.org/10.1101/cshperspect.a005637.
[25] N.L. Smith, M.H. Chen, A. Dehghan, D.P. Strachan, S. Basu, N. Soranzo, C. Hayward, I. Rudan, M. Sabater-Lleal, J.C. Bis, M.P.M. De Maat, A. Rumley, X. Kong, Q. Yang, F.M.K. Williams, V. Vitart, H. Campbell, A. Mälarstig, K.L. Wiggins, C.M. Van Duijn, W.L. McArdle, J.S. Pankow, A.D. Johnson, A. Silveira, B. McKnight, A.G. Uitterlinden, N. Aleksic, J.B. Meigs, A. Peters, W. Koenig, M. Cushman, S. Kathiresan, J.I. Rotter, E.G. Bovill, A. Hofman, E. Boerwinkle, G.H. Tofler, J.F. Peden, B.M. Psaty, F. Leebeek, A.R. Folsom, M.G. Larson, T.D. Spector, A.F. Wright, J.F. Wilson, A. Hamsten, T. Lumley, J.C.M. Witteman, W. Tang, C.J. O'Donnell, Novel associations of multiple genetic loci with plasma levels of factor VII, factor VIII, and von willebrand factor: the charge (cohorts for heart and aging research in genome epidemiology) consortium, Circulation 121 (2010) 1382–1392, https://doi.org/10.1161/CIRCULATIONAHA.109.869156.
[26] J.E. van Loon, F.W.G. Leebeek, J.W. Deckers, D.W.J. Dippel, D. Poldermans, D.P. Strachan, W. Tang, C.J. O'Donnell, N.L. Smith, M.P.M. de Maat, Effect of genetic variations in syntaxin-binding protein-5 and syntaxin-2 on von Willebrand factor concentration and cardiovascular risk, Circ. Cardiovasc. Genet. 3 (2010) 507–512, https://doi.org/10.1161/CIRCGENETICS.110.957407.
[27] M. Schillemans, E. Karampini, B.L. van den Eshof, A. Gangaev, M. Hofman, D. van Breevoort, H. Meems, H. Janssen, A.A. Mulder, C.R. Jost, J.C. Escher, R. Adam, T. Carter, A.J. Koster, M. van den Biggelaar, J. Voorberg, R. Bierings, Weibel-Palade body localized Syntaxin-3 modulates Von Willebrand factor secretion from endothelial cells, Arterioscler. Thromb. Vasc. Biol. 38 (2018) 1549–1561, https://doi.org/10.1161/ATVBAHA.117.310701.
[28] J. Fu, A.P. Naren, X. Gao, G.U. Ahmmed, A.B. Malik, Protease-activated receptor-1 activation of endothelial cells induces protein kinase Calpha-dependent phosphorylation of syntaxin 4 and Munc18c: role in signaling p-selectin expression, J. Biol. Chem. 280 (2005) 3178–3184 (doi:M410044200 [pii] 10.1074/jbc.M410044200).

[29] Q.M. Zhu, Q. Zhu, M. Yamakuchi, C.J. Lowenstein, SNAP23 regulates endothelial exocytosis of von Willebrand factor, PLoS ONE 10 (2015) e0118737, , https://doi.org/10.1371/journal.pone.0118737.
[30] I.R. Pulido, R. Jahn, V. Gerke, VAMP3 is associated with endothelial Weibel-Palade bodies and participates in their ca(2+)-dependent exocytosis, Biochim. Biophys. Acta 1813 (2011) 1038–1044, https://doi.org/10.1016/j.bbamcr.2010.11.007.
[31] E. Karampini, M. Schillemans, M. Hofman, F. van Alphen, M. de Boer, T.W. Kuijpers, M. van den Biggelaar, J. Voorberg, R. Bierings, Defective AP-3-dependent VAMP8 trafficking impairs Weibel-Palade body exocytosis in Hermansky-Pudlak syndrome type 2 blood outgrowth endothelial cells, Haematologica (2019), https://doi.org/10.3324/haematol.2018.207787.
[32] D. van Breevoort, A.P. Snijders, N. Hellen, S. Weckhuysen, K.W.E.M. van Hooren, J. Eikenboom, K. Valentijn, M. Fernandez-Borja, B. Ceulemans, P. De Jonghe, J. Voorberg, M. Hannah, T. Carter, R. Bierings, STXBP1 promotes Weibel-Palade body exocytosis through its interaction with the Rab27A effector Slp4-a, Blood. 123 (2014) 3185–3194, https://doi.org/10.1182/blood-2013-10-535831.
[33] J. Rizo, T.C. Sudhof, Snares and Munc18 in synaptic vesicle fusion, Nat. Rev. Neurosci. 3 (2002) 641–653, https://doi.org/10.1038/nrn898.
[34] Q. Zhu, M. Yamakuchi, S. Ture, M. de la Luz Garcia-Hernandez, K.A. Ko, K.L. Modjeski, M.B. LoMonaco, A.D. Johnson, C.J. O'Donnell, Y. Takai, C.N. Morrell, C.J. Lowenstein, Syntaxin-binding protein STXBP5 inhibits endothelial exocytosis and promotes platelet secretion, J. Clin. Invest. 124 (2014) 4503–4516, https://doi.org/10.1172/JCI71245.
[35] G. Antoni, T. Oudot-Mellakh, A. Dimitromanolakis, M. Germain, W. Cohen, P. Wells, M. Lathrop, F. Gagnon, P.E. Morange, D.A. Tregouet, Combined analysis of three genome-wide association studies on vWF and FVIII plasma levels, BMC Med. Genet. 12 (2011) 102, , https://doi.org/10.1186/1471-2350-12-102.
[36] J.E. van Loon, Y.V. Sanders, E.M. de Wee, M.J.H. a Kruip, M.P.M. de Maat, F.W.G. Leebeek, Effect of genetic variation in STXBP5 and STX2 on von Willebrand factor and bleeding phenotype in type 1 von Willebrand disease patients, PLoS ONE 7 (2012) e40624, , https://doi.org/10.1371/journal.pone.0040624.
[37] Y.V. Sanders, J.G. van der Bom, A. Isaacs, M.H. Cnossen, M.P.M. de Maat, B.A.P. Laros-van Gorkom, K. Fijnvandraat, K. Meijer, C.M. van Duijn, E.P. Mauser-Bunschoten, J. Eikenboom, F.W.G. Leebeek, WiN study group, CLEC4M and STXBP5 gene variations contribute to von Willebrand factor level variation in von Willebrand disease, J. Thromb. Haemost. 13 (2015) 956–966, https://doi.org/10.1111/jth.12927.
[38] J. Van Loon, A. Dehghan, T. Weihong, S. Trompet, W.L. McArdle, F.W. Asselbergs, M.-H.H. Chen, L.M. Lopez, J.E. Huffman, F.W.G.G. Leebeek, S. Basu, D.J. Stott, A. Rumley, R.T. Gansevoort, G. Davies, J.J.F.F. Wilson, J.C.M.M. Witteman, X. Cao, A.J.M.M. de Craen, S.J.L.L. Bakker, B.M. Psaty, J.M. Starr, A. Hofman, J. Wouter Jukema, I.J. Deary, C. Hayward, P. Van Der Harst, G.D.O.O. Lowe, A.R. Folsom, D.P. Strachan, N. Smith, M.P.M.M. De Maat, C. O'Donnell, J.W. Jukema, I.J. Deary, C. Hayward, P. Van Der Harst, G.D.O.O. Lowe, A.R. Folsom, D.P. Strachan, N. Smith, M.P.M.M. De Maat, C. O'Donnell, Genome-wide association studies identify genetic loci for low von Willebrand factor levels, Eur. J. Hum. Genet. 24 (2016) 1035–1040, https://doi.org/10.1038/ejhg.2015.222.
[39] C. Lind-Halldén, E. Manderstedt, D. Carlberg, S. Lethagen, C. Halldén, Genetic variation in the Syntaxin-binding protein STXBP5 in type 1 von Willebrand disease patients, Thromb. Haemost. 118 (2018) 1382–1389, https://doi.org/10.1055/s-0038-1661352.
[40] N.L. Smith, K.M. Rice, E.G. Bovill, M. Cushman, J.C. Bis, B. McKnight, T. Lumley, N.L. Glazer, A. van Hylckama Vlieg, W. Tang, A. Dehghan, D.P. Strachan, C.J. O'Donnell, J.I. Rotter, S.R. Heckbert, B.M. Psaty, F.R. Rosendaal, Genetic variation associated with plasma von Willebrand factor levels and the risk of incident venous thrombosis, Blood. 117 (2011) 6007–6011, https://doi.org/10.1182/blood-2010-10-315473.
[41] R.H. Kutner, X.-Y. Zhang, J. Reiser, Production, concentration and titration of pseudotyped HIV-1-based lentiviral vectors, Nat. Protoc. 4 (2009) 495–505, https://doi.org/10.1038/nprot.2009.22.
[42] S. Tyanova, T. Temu, J. Cox, The MaxQuant computational platform for mass spectrometry-based shotgun proteomics, Nat. Protoc. (2016), https://doi.org/10.1038/nprot.2016.136.
[43] W. Huber, V.J. Carey, R. Gentleman, S. Anders, M. Carlson, B.S. Carvalho, H.C. Bravo, S. Davis, L. Gatto, T. Girke, R. Gottardo, F. Hahne, K.D. Hansen, R.A. Irizarry, M. Lawrence, M.I. Love, J. MaCdonald, V. Obenchain, A.K. Oleś, H. Pagès, A. Reyes, P. Shannon, G.K. Smyth, D. Tenenbaum, L. Waldron, M. Morgan, Orchestrating high-throughput genomic analysis with Bioconductor, Nat. Methods (2015), https://doi.org/10.1038/nmeth.3252.
[44] M.E. Ritchie, B. Phipson, D. Wu, Y. Hu, C.W. Law, W. Shi, G.K. Smyth, Limma powers differential expression analyses for RNA-sequencing and microarray studies, Nucleic Acids Res. (2015), https://doi.org/10.1093/nar/gkv007.
[45] M.Y. Hein, N.C. Hubner, I. Poser, J. Cox, N. Nagaraj, Y. Toyoda, I.A. Gak, I. Weisswange, J. Mansfeld, F. Buchholz, A.A. Hyman, M. Mann, A human Interactome in three quantitative dimensions organized by Stoichiometries and abundances, Cell. 163 (2015) 712–723, https://doi.org/10.1016/j.cell.2015.09.053.
[46] J.A. Vizcaíno, E.W. Deutsch, R. Wang, A. Csordas, F. Reisinger, D. Ríos, J.A. Dianes, Z. Sun, T. Farrah, N. Bandeira, P.-A. Binz, I. Xenarios, M. Eisenacher, G. Mayer, L. Gatto, A. Campos, R.J. Chalkley, H.-J. Kraus, J.P. Albar, S. Martinez-Bartolomé, R. Apweiler, G.S. Omenn, L. Martens, A.R. Jones, H. Hermjakob, ProteomeXchange provides globally coordinated proteomics data submission and dissemination, Nat. Biotechnol. 32 (2014) 223–226, https://doi.org/10.1038/nbt.2839.
[47] R. Oughtred, C. Stark, B.-J. Breitkreutz, J. Rust, L. Boucher, C. Chang, N. Kolas, L. O'Donnell, G. Leung, R. McAdam, F. Zhang, S. Dolma, A. Willems, J. Coulombe-Huntington, A. Chatr-Aryamontri, K. Dolinski, M. Tyers, The BioGRID interaction database: 2019 update, Nucleic Acids Res. 47 (2019) D529–D541, https://doi.org/10.1093/nar/gky1079.
[48] R. Al Hawas, Q. Ren, S. Ye, Z.A. Karim, A.H. Filipovich, S.W. Whiteheart, Munc18b/STXBP2 is required for platelet secretion, Blood 120 (2012) 2493–2500, https://doi.org/10.1182/blood-2012-05-430629.
[49] C.L. Wiegerinck, A.R. Janecke, K. Schneeberger, G.F. Vogel, D.Y. van Haaften-Visser, J.C. Escher, R. Adam, C.E. Thöni, K. Pfaller, A.J. Jordan, C.-A. Weis, I.J. Nijman, G.R. Monroe, P.M. van Hasselt, E. Cutz, J. Klumperman, H. Clevers, E.E.S. Nieuwenhuis, R.H.J. Houwen, G. van Haaften, M.W. Hess, L. a Huber, J.M. Stapelbroek, T. Müller, S. Middendorp, Loss of syntaxin 3 causes variant microvillus inclusion disease, Gastroenterology. 147 (2014) 65–68.e10, , https://doi.org/10.1053/j.gastro.2014.04.002.
[50] M. Steegmaier, E. Borges, J. Berger, H. Schwarz, D. Vestweber, The E-selectin-ligand ESL-1 is located in the Golgi as well as on microvilli on the cell surface, J. Cell Sci. 110 (Pt 6) (1997) 687–694 http://www.ncbi.nlm.nih.gov/pubmed/9099943.
[51] D. Fasshauer, R.B. Sutton, A.T. Brunger, R. Jahn, Conserved structural features of the synaptic fusion complex: SNARE proteins reclassified as Q- and R-SNAREs, Proc. Natl. Acad. Sci. 95 (1998) 15781–15786, https://doi.org/10.1073/pnas.95.26.15781.
[52] E.S. Masuda, B.C.B. Huang, J.M. Fisher, Y. Luo, R.H. Schneller, R.H. Scheller, Tomosyn binds t-SNARE proteins via a VAMP-like coiled coil, Neuron 21 (1998) 479–480, https://doi.org/10.1590/S2317-17822013000500002.
[53] Y. Fujita, H. Shirataki, T. Sakisaka, T. Asakura, T. Ohya, H. Kotani, S. Yokoyama, H. Nishioka, Y. Matsuura, A. Mizoguchi, R.H. Scheller, Y. Takai, Tomosyn: a Syntaxin-1–binding protein that forms a novel complex in the neurotransmitter release process, Neuron. 20 (1998) 905–915, https://doi.org/10.1016/S0896-6273(00)80472-9.
[54] S. Ye, Y. Huang, S. Joshi, J. Zhang, F. Yang, G. Zhang, S.S. Smyth, Z. Li, Y. Takai, S.W. Whiteheart, Platelet secretion and hemostasis require syntaxin-binding protein STXBP5, J. Clin. Invest. 124 (2014) 4517–4528, https://doi.org/10.1172/JCI75572.
[55] T. Yamaguchi, I. Dulubova, S.-W. Min, X. Chen, J. Rizo, T.C. Südhof, Sly1 binds to Golgi and ER Syntaxins via a conserved N-terminal peptide motif, Dev. Cell 2 (2002) 295–305, https://doi.org/10.1016/S1534-5807(02)00125-9.
[56] M. Tagaya, K. Arasaki, H. Inoue, H. Kimura, Moonlighting functions of the NRZ (mammalian Dsl1) complex, Front. Cell Dev. Biol. 2 (2014) 25, , https://doi.org/10.3389/fcell.2014.00025.
[57] A.V. Pobbati, A. Razeto, M. Böddener, S. Becker, D. Fasshauer, Structural basis for the inhibitory role of tomosyn in exocytosis, J. Biol. Chem. 279 (2004) 47192–47200, https://doi.org/10.1074/jbc.M408767200.
[58] W. Zhang, L. Lilja, S.A. Mandic, J. Gromada, K. Smidt, J. Janson, Y. Takai, C. Bark, P.-O. Berggren, B. Meister, Tomosyn is expressed in -cells and negatively regulates insulin exocytosis, Diabetes. 55 (2006) 574–581, https://doi.org/10.2337/diabetes.55.03.06.db05-0015.
[59] S.E. Gladycheva, A.D. Lam, J. Liu, M. D'Andrea-Merrins, O. Yizhar, S.I. Lentz, U. Ashery, S. a Ernst, E.L. Stuenkel, Receptor-mediated regulation of tomosyn-syntaxin 1A interactions in bovine adrenal chromaffin cells, J. Biol. Chem. 282 (2007) 22887–22899, https://doi.org/10.1074/jbc.M701787200.
[60] T. Sakisaka, Y. Yamamoto, S. Mochida, M. Nakamura, K. Nishikawa, H. Ishizaki, M. Okamoto-Tanaka, J. Miyoshi, Y. Fujiyoshi, T. Manabe, Y. Takai, Dual inhibition of SNARE complex formation by tomosyn ensures controlled neurotransmitter release, J. Cell Biol. 183 (2008) 323–337, https://doi.org/10.1083/jcb.200805150.
[61] Y. Yamamoto, S. Mochida, T. Kurooka, T. Sakisaka, Reciprocal intramolecular interactions of tomosyn control its inhibitory activity on SNARE complex formation, J. Biol. Chem. 284 (2009) 12480–12490, https://doi.org/10.1074/jbc.M807182200.
[62] Y. Yamamoto, K. Fujikura, M. Sakaue, K. Okimura, Y. Kobayashi, T. Nakamura, T. Sakisaka, The tail domain of tomosyn controls membrane fusion through tomosyn displacement by VAMP2, Biochem. Biophys. Res. Commun. 399 (2010) 24–30, https://doi.org/10.1016/j.bbrc.2010.07.026.
[63] Y. Yamamoto, S. Mochida, N. Miyazaki, K. Kawai, K. Fujikura, T. Kurooka, K. Iwasaki, T. Sakisaka, Tomosyn inhibits synaptotagmin-1-mediated step of Ca2+ −dependent neurotransmitter release through its N-terminal WD40 repeats, J. Biol. Chem. 285 (2010) 40943–40955, https://doi.org/10.1074/jbc.M110.156893.
[64] E.O. Gracheva, E.B. Maryon, M. Berthelot-Grosjean, J.E. Richmond, Differential regulation of synaptic vesicle tethering and docking by UNC-18 and TOM-1, Front. Synaptic Neurosci. 2 (2010) 141, , https://doi.org/10.3389/fnsyn.2010.00141.
[65] K. Hatsuzawa, T. Lang, D. Fasshauer, D. Bruns, R. Jahn, The R-SNARE motif of tomosyn forms SNARE core complexes with syntaxin 1 and SNAP-25 and down-regulates exocytosis, J. Biol. Chem. 278 (2003) 31159–31166, https://doi.org/10.1074/jbc.M305500200.
[66] Q.M. Zhu, K.A. Ko, S. Ture, M.A. Mastrangelo, M.-H. Chen, A.D. Johnson, C.J. O'Donnell, C.N. Morrell, J.M. Miano, C.J. Lowenstein, Novel thrombotic function of a human SNP in STXBP5 revealed by CRISPR/Cas9 gene editing in mice, Arterioscler. Thromb. Vasc. Biol. 37 (2017) 264–270, https://doi.org/10.1161/ATVBAHA.116.308614.
[67] S. Takeuchi, S. Iwama, H. Takagi, A. Kiyota, K. Nakashima, H. Izumida, H. Fujisawa, N. Iwata, H. Suga, T. Watanabe, K. Kaibuchi, Y. Oiso, H. Arima, Y. Sugimura, Tomosyn negatively regulates arginine vasopressin secretion in embryonic stem cell-derived neurons, PLoS ONE 11 (2016) 1–21, https://doi.org/10.1371/journal.pone.0164544.
[68] E.L. Huttlin, R.J. Bruckner, J.A. Paulo, J.R. Cannon, L. Ting, K. Baltier, G. Colby, F. Gebreab, M.P. Gygi, H. Parzen, J. Szpyt, S. Tam, G. Zarraga, L. Pontano-Vaites, S. Swarup, A.E. White, D.K. Schweppe, R. Rad, B.K. Erickson, R.A. Obar, K.G. Guruharsha, K. Li, S. Artavanis-Tsakonas, S.P. Gygi, J.W. Harper, J. Wade

Harper, J.W. Harper, J. Wade Harper, Architecture of the human interactome defines protein communities and disease networks, Nature. 545 (2017) 505–509, https://doi.org/10.1038/nature22366.

[69] I.K. Madera-Salcedo, L. Danelli, N. Tiwari, B. Dema, E. Pacreau, S. Vibhushan, J. Birnbaum, C. Agabriel, V. Liabeuf, C. Klingebiel, G. Menasche, M. Macias-Silva, M. Benhamou, N. Charles, C. González-Espinosa, J. Vitte, U. Blank, Tomosyn functions as a PKC-regulated fusion clamp in mast cell degranulation, Sci. Signal. 11 (2018) 1–12, https://doi.org/10.1126/scisignal.aan4350.

[70] C.H. Widberg, N.J. Bryant, M. Girotti, S. Rea, D.E. James, Tomosyn interacts with the t-SNAREs syntaxin4 and SNAP23 and plays a role in insulin-stimulated GLUT4 translocation, J. Biol. Chem. 278 (2003) 35093–35101, https://doi.org/10.1074/jbc.M304261200.

[71] N. Bielopolski, A.D. Lam, D. Bar-On, M. Sauer, E.L. Stuenkel, U. Ashery, Differential interaction of tomosyn with syntaxin and SNAP25 depends on domains in the WD40 beta-propeller core and determines its inhibitory activity, J. Biol. Chem. (2014), https://doi.org/10.1074/jbc.M113.515296.

[72] O. Yizhar, N. Lipstein, S.E. Gladycheva, U. Matti, S.A. Ernst, J. Rettig, E.L. Stuenkel, U. Ashery, Multiple functional domains are involved in tomosyn regulation of exocytosis, J. Neurochem. 103 (2007) 604–616, https://doi.org/10.1111/j.1471-4159.2007.04791.x.

[73] C.J. Geerts, R. Mancini, N. Chen, F.T.W. Koopmans, K.W. Li, A.B. Smit, J.R.T. van Weering, M. Verhage, A.J.A. Groffen, Tomosyn associates with secretory vesicles in neurons through its N- and C-terminal domains, PLoS ONE 12 (2017) e0180912, , https://doi.org/10.1371/journal.pone.0180912.

[74] C. Lenzi, J. Stevens, D. Osborn, M.J. Hannah, R. Bierings, T. Carter, Synaptotagmin 5 regulates Ca2 + − dependent Weibel-Palade body exocytosis in human endothelial cells, J. Cell Sci. 132 (2019), https://doi.org/10.1242/jcs.221952.